HYDROLOGICAL PROCESSES
Hydrol. Process. (2007)
Published online in Wiley InterScience
(www.interscience.wiley.com) DOI: 10.1002/hyp.6891

Automatic mapping of snow cover depletion curves using optical remote sensing data under conditions of frequent cloud cover and temporary snow

Baolin Li,[1]* A-Xing Zhu,[1,2] Chenghu Zhou,[1] Yichi Zhang,[1] Tao Pei[1] and Chengzhi Qin[1]

[1] *State Key Lab of Resources and Environmental Information System, Institute of Geographical Sciences and Natural Resources Research, Chinese Academy of Sciences, No. 11 Datun Road, An Wai, Beijing 100101, China*
[2] *Department of Geography, University of Wisconsin, 550 North Park Street, Madison, Wisconsin 53706, USA*

Abstract:

Snow cover depletion curves are required for several water management applications of snow hydrology and are often difficult to obtain automatically using optical remote sensing data owing to both frequent cloud cover and temporary snow cover. This study develops a methodology to produce accurate snow cover depletion curves automatically using high temporal resolution optical remote sensing data (e.g. Terra Moderate Resolution Imaging Spectroradiometer (MODIS), Aqua MODIS or National Oceanic and Atmospheric Administration (NOAA) Advanced Very High Resolution Radiometer (AVHRR)) by snow cover change trajectory analysis. The method consists of four major steps. The first is to reclassify both cloud-obscured land and snow into more distinct subclasses and to determine their snow cover status (seasonal snow cover or not) based on the snow cover change trajectories over the whole snowmelt season. The second step is to derive rules based on the analysis of snow cover change trajectories. These rules are subsequently used to determine for a given date, the snow cover status of a pixel based on snow cover maps from the beginning of the snowmelt season to that given date. The third step is to apply a decision-tree-like processing flow based on these rules to determine the snow cover status of a pixel for a given date and to create daily seasonal snow cover maps. The final step is to produce snow cover depletion curves using these maps. A case study using this method based on Terra MODIS snow cover map products (MOD10A1) was conducted in the lower and middle reaches of the Kaidu River Watershed (19 000 km^2) in the Chinese Tien Shan, Xinjiang Uygur Autonomous Region, China. High resolution remote sensing data (charge coupled device (CCD) camera data with 19·5 m resolution of the China and Brazil Environmental and Resources Satellite (CBERS) data (19·5 m resolution), and the Advanced Spaceborne Thermal Emission and Reflection Radiometer (ASTER) data with 15 m resolution of the Terra) were used to validate the results. The study shows that the seasonal snow cover classification was consistent with that determined using a high spatial resolution dataset, with an accuracy of 87–91%. The snow cover depletion curves clearly reflected the impact of the variation of temperature and the appearance of temporary snow cover on seasonal snow cover. The findings from this case study suggest that the approach is successful in generating accurate snow cover depletion curves automatically under conditions of frequent cloud cover and temporary snow cover using high temporal resolution optical remote sensing data.

KEY WORDS snow cover depletion curves; seasonal snow cover; temporary snow cover; high temporal resolution optical remote sensing data; snow cover change trajectory; snow runoff model

Received 30 March 2007; Accepted 17 August 2007

INTRODUCTION

Snow cover can be grouped into two categories: seasonal snow cover and temporary snow cover (Hall and Martinec, 1985). Seasonal snow cover is formed by consecutive snowfall during the snow-accumulation season and gradually disappears during the snowmelt season. Temporary snow cover, which can also be specified as short-lived snow (WinSRM, 2003), is formed by a snowstorm during the snowmelt season, and exists only for a number hours or a few days. Snow cover depletion curves based on seasonal snow cover maps are frequently required for several water-management applications of snow hydrology (Martinec, 1975; Martinec and Rango, 1986; Engman and Gurney, 1991; Shamir and Georgakakos, 2007).

Snow cover depletion curves are commonly obtained by interpolating percentages of snow cover area for dates when cloud free and temporary snow free scenes are available. This method, however, has two problems: (1) low efficiency and (2) low accuracy.

The low efficiency of mapping snow cover depletion curves is mainly related to the process of determining cloud free and temporary snow cover free scenes. The selection of these images is generally performed through comparison of images from different dates with coincidental precipitation and temperature data via visual interpretation (Baumgartner *et al*., 1987; Baumgartner and Rango, 1995), which is often with low efficiency.

The low accuracy of this method is caused by: (1) the method of determining the cloud free and temporarily

* Correspondence to: Baolin Li, State Key Lab of Resources and Environmental Information System, Institute of Geographical Sciences and Natural Resources Research, Chinese Academy of Sciences, No. 11 Datun Road, An Wai, Beijing 100101, China. E-mail: libl@lreis.ac.cn

snow cover free scenes; and (2) the coarse temporal resolution of these data. Determining whether a scene is cloud free or temporarily snow cover free is based on visual interpretation. Thus, the determination of temporarily snow cover free scenes is subjective. Therefore, in this category, images with some temporary snow cover may be occasionally selected. This margin of error will therefore cause errors in snow cover depletion curves (Hall and Martinec, 1985).

The current temporal resolution of cloud free and temporary snow cover free scenes is often longer than a week in snow cover depletion curve applications because of the limited availability of such scenes (Akyürek and Sorman, 2002; WinSRM, 2003; Tekeli *et al.*, 2005). The coarse temporal resolution causes the interpolated snow cover depletion curves to fail to reflect detailed snow cover depletion process (Schaper *et al*, 1999).

When temporary snow cover blankets seasonal snow cover, seasonal snow cover should stop melting (WinSRM, 2003). Seasonal snow will have been melting up until the snowfall event. Thus, the snow cover depletion curves can generally be characterized by a concave shape. Interpolated snow cover depletion curves cannot capture this information.

To solve the problems of the commonly-used interpolation methods of mapping snow cover depletion curves, much research has been conducted. The issue of cloud cover and temporary snow cover are the two major obstacles to mapping snow cover depletion curves using optical remote sensing data, so most research has focused on how to overcome these two obstacles.

To solve the first problem, two main methods are used. The first is to use microwave remote sensing data to detect snow cover under cloud. Microwave remote sensing includes data from both passive and active instruments. The spatial resolutions of passive microwave data such as the Scanning Multichannel Microwave Radiometer (SMMR), the Special Sensor Microwave/Imager (SSM/I) and Advanced Microwave Scanning Radiometer (AMSR-E) are very coarse, with spatial resolutions of 25 km or 10 km (Mognard *et al.*, 2004). The coarse spatial resolution restricts their use in snow cover mapping (Rango, 1996). Active microwave data with higher spatial resolution, such as Envisat Advanced Synthetic Aperture Radar (ASAR) and Radarsat and European Remote Sensing Satellite (ERS) can detect snow cover under cloud easily (Nagler and Rott, 1998; Koskinen *et al.*, 1999; Guneriussen *et al.*, 2001; Guneriussen and Johnsen, 2003; Storvold and Malnes, 2004). However, these SAR generally cannot detect dry snow and their temporal resolutions, ranging from 24 to 35 days, are too low, and thus cannot be used for the purpose of mapping detailed snow cover depletion curves.

The second method involves extrapolating snow cover over a cloud-obscured area. This method assumes that a certain basin area is exposed to the same process of snow deposition and depletion; the snow cover ratio for a landform class (having the same range of elevation, slope and aspect) is similar in the entire basin (Seidel *et al.*, 1983). The snow cover ratio is computed for each landform class in the cloud-free area (reference area) and then extrapolated to the same landform class in the cloud-obscured area (Seidel *et al.*, 1983; Baumgartner *et al.*, 1986). The total snow cover includes both the snow cover in the cloud-free area and that extrapolated in the cloud-obscured area. When this method is used, the reference area in the cloud-free region must be large enough to be representative of the conditions of the cloud-obscured area. However, the serious cloud contamination in alpine mountains usually causes the cloud-free area to be very limited (Ranzi *et al.*, 1999). This will impact strongly on the accuracy of snow cover extrapolation.

There are currently no effective methods to deal with the second obstacle (temporary snow cover) when mapping snow cover depletion curves. Owing to their spectral similarity as well as the inability of optical sensors to penetrate temporary snow cover (Hall and Martinec, 1985), we cannot map seasonal snow cover under temporary snow using optical remote sensing techniques. As a result, images with temporary snow cover are not used when producing snow cover depletion curves (WinSRM, 2003).

As discussed above, there are no effective methods to acquire frequent seasonal snow cover maps so that accurate snow cover depletion curves can be produced automatically. The goal of the proposed methodology is to distinguish seasonal snow cover from other land-cover types, including temporary snow cover and cloud cover, based on the analysis of snow cover change trajectories using optical remote sensing data with high temporal resolution. The pixel-wise analysis consists of three steps: (1) identifying the snow cover trajectory time series based on the three classes defined in a later section; (2) reclassification of those three classes each time into subclasses based on the temporal sequence of classes; and (3) determining the snow cover status (seasonal snow or not seasonal snow). Using this method, temporary snow cover can be eliminated and seasonal snow cover in cloud-obscured areas can be directly extrapolated. Thus, accurate snow cover depletion curves can be produced automatically.

METHODOLOGY

Study Area and Data

Study area. The study area is between 82°8′–86°55′E and 41°47′–43°21′N, in Xinjiang Uygur Autonomous Region, China, and is in the Kaidu River Watershed of the Chinese Tien Shan to the north of the Tarim Basin (Figure 1). The source of the river is the Sharming Peak of the Chinese Tien Shan. The main stream flows from east to west through the Small Yoerdos Basin, then turns south-east at Bayanblak and passes through the Large Yoerdos Basin. The study area covers about 19 000 km^2. The relief of the watershed is very complex, composed of high peaks, deep valleys and shallow basins with elevation decreasing from the north to the south.

DOI: 10.1002/hyp

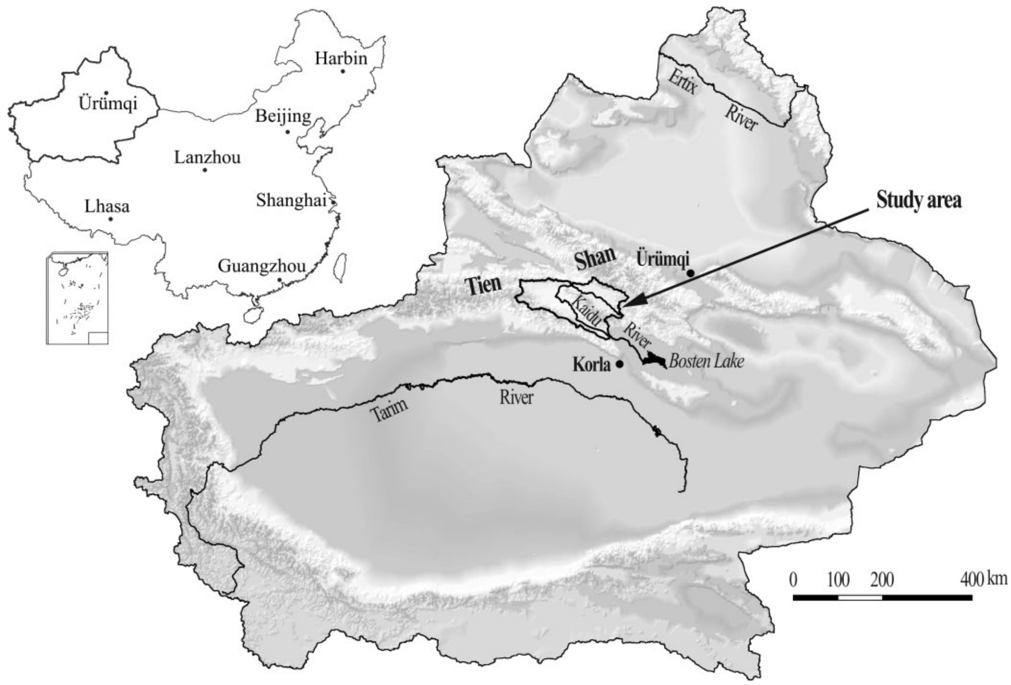

Figure 1. Location of the study area

Snowmelt runoff provides the main source of water for the oases at the foothills of the Chinese Tien Shan during spring. The oases in these areas have become some of the most developed regions in China's arid zones, and have been regarded as some of the most successful development areas in China's Xinjiang Uygur Autonomous Region. Therefore, snowmelt runoff as a water source for agriculture and industry is very important for the development of the local economy.

Data and data preprocessing. Terra MODIS snow cover maps are used as inputs for mapping seasonal snow cover. Terra MODIS Snow Cover Daily L3 Global 500 m Grid (MOD10A1) data from 15 March to 10 June between 2000 and 2005 were acquired. The pixel values of the MOD10A1 data in the study area include 1 (No decision), 25 (Snow-free land), 50 (Cloud obscured), 200 (Snow) and 254 (Detector saturated) (Riggs *et al.*, 2006; Hall and Riggs, 2007). The surface land cover on pixels denoted 'No decision' and 'Detector saturated' cannot be determined, so these pixels are combined with those of 'Cloud obscured'. Thus, the surface land cover of snow cover maps are recoded into three classes in this study: snow, cloud-obscured land and snow-free land. According to the statistics in the study area, the percentages of 'No decision' pixels or 'Detector saturated' pixels on most snow cover maps are less than 1%. Therefore, the impact of these two kinds of pixels on seasonal snow cover mapping will be limited in this study.

Five high spatial resolution (15–30 m) remote sensing data sets (Table I) were used to assess the accuracy of these snow cover maps. These accuracy measures serve as a benchmark for assessing the quality of the approach presented later in this paper. The five remote sensing data sets include three scenes from the China and Brazil Environmental and Resources Satellite (CBERS), the Charge Coupled Device Camera (CCD) data, one scene from Terra, the Advanced Spaceborne Thermal Emission and Reflection Radiometer (ASTER) data and one scene from Landsat, Enhanced Thematic Mapper Plus (ETM+) data (Table I). They were all registered based on topographical maps at a scale of 1 : 100 000. The largest RMS errors were less than 1·5 pixels. ASTER and CBERS images were also used to validate the seasonal snow maps produced using the method described in this paper.

The overall accuracy and kappa index based on the confusion matrix were used as accuracy measures to assess the accuracies of the MODIS snow cover maps. The confusion matrix gives results of a comparison of the classified images with reference data. Overall accuracy measures the percentage of correctly classified samples in the reference data. The kappa index is a measure of the difference between actual agreement and chance agreement between remotely sensed classification and reference data. For details refer to Congalton and Green (1999). A stratified random sampling scheme was used to obtain samples. No samples were taken from areas covered by cloud, either on the snow cover map or

Table I. Remote sensing data used for validation

Satellite	Sensor	Resolution (m)	Acquisition Date
CBERS 1	CCD	19·5	27/03/2001
CBERS 1	CCD	19·5	12/05/2001
CBERS 2	CCD	19·5	01/06/2004
Terra	ASTER	15	22/05/2001
Landsat 7	ETM+	30	10/05/2000

Table II. Accuracies of MODIS snow cover maps

Accuracy	10/05/2000	27/03/2001	12/05/2001	22/05/2001	01/06/2004
Overall accuracy	92%	89%	87%	88%	96%
Kappa index	0·76	0·78	0·64	0·76	0·81

on the validation imagery. 200 samples based on a stratified random sampling scheme were collected for this assessment.

Table II shows the high accuracies of the MODIS snow cover maps, with overall accuracy ranging from 87 to 96%. The kappa index varies from 0·64 to 0·81. The high accuracy of these snow cover maps indicates that the impact of snow cover misclassification on seasonal snow cover mapping will be limited in this study.

Snow cover change trajectory analysis

The general idea of this method is that the existence of snow cover on some dates at a site can provide prior information for determining the presence of snow cover on other dates at the same site. According to an analysis of snow cover change trajectories, the snow cover status for a pixel on a given date can be determined by using snow cover maps from the beginning of the snowmelt season to the given date.

The concept of snow cover change trajectory. The concept of land cover change trajectory was developed by Mertens and Lambin (2000) and Petit *et al.* (2001). The concept generally refers to the succession of land cover types for a given sample unit over more than two observations. The snow cover change trajectory in this study similarly reflects this concept. The surface land cover in this study includes three types: snow, cloud-obscured land and snow-free land. The snow cover change trajectory refers to succession of the above three surface land cover types on a pixel.

For simplicity in describing the concept, the period between the study area's maximum snow cover date and the seasonal snow cover melting completion date (the whole snowmelt season) is used as an example. The maximum snow cover appears 10–31 March and seasonal snow cover melting terminates on 20 May to 10 June in the study area (Ma, 2002). The entire snowmelt season is included in the analysis, thus, the focus is on the succession between 15 March and 10 June, giving a total of 88 observations in this study.

All possible snow cover change trajectories during the whole snowmelt season are shown in Figure 2. For example, a snow cover change trajectory (thick lines) can be specified as $S^{3\cdot15} \rightarrow \ldots \rightarrow S^{4\cdot19} \rightarrow S^{4\cdot20} \rightarrow L^{4\cdot21} \rightarrow L^{4\cdot22} \rightarrow \ldots \rightarrow L^{6\cdot9} \rightarrow L^{6\cdot10}$, which means that the pixel is covered by snow from 15 March to 20 April, snow cover melts completely on 21 April and this pixel is no longer snow-covered or cloud-obscured from 21 April to 10 June.

Reclassification of both snow and cloud-obscured land. Both snow and cloud-obscured land are reclassified according to the sequence of appearance dates of both snow and cloud-obscured land and the first appearance date of snow-free land. Two classification trees are used to perform this process (Figure 3). Finally, obscured-land is reclassified into four classes and snow is reclassified into three classes (Figure 3, Table III).

$Cloud_{after}$ occurs after the first appearance date of snow-free land (C_{after} in the trajectory example of Table III, Figure 3). Subscript 'after' denotes the fact that the cloud-obscured land occurs 'after' the first appearance date of snow-free land.

$Cloud_{before\_c}$ occurs before the first appearance date of snow-free land in a trajectory and only cloud-obscured land occurs before the appearance date of the $Cloud_{before\_c}$ (C_{before_c} in the trajectory example of Table III, Figure 3). Subscript 'before' denotes the fact that cloud-obscured land occurs before the first appearance date of snow-free land and subscript 'c' deontes the fact that 'only cloud-obscured land' exists before the appearance date of the $Cloud_{before\_c}$.

$Cloud_{before\_ss}$ occurs before the first appearance date of snow-free land in a trajectory. At the same time, some snow occurs before the appearance date of the $Cloud_{before\_ss}$ and some snow also occurs between the appearance date of the $Cloud_{before\_ss}$ and the first appearance date of snow-free land (C_{before_ss} in the trajectory example in Table III, Figure 3). Subscript 'before'

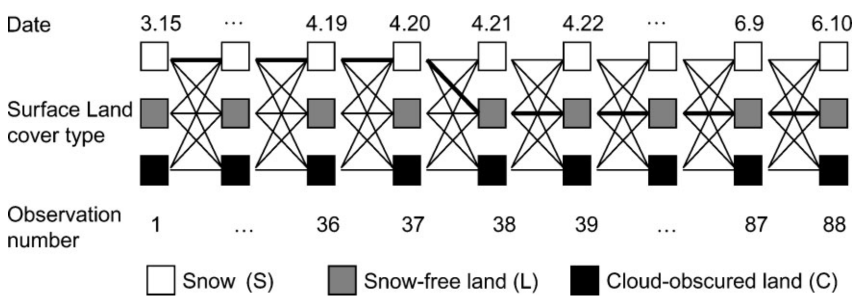

Figure 2. All possible snow cover change trajectories over the whole snowmelt season in this study

DOI: 10.1002/hyp

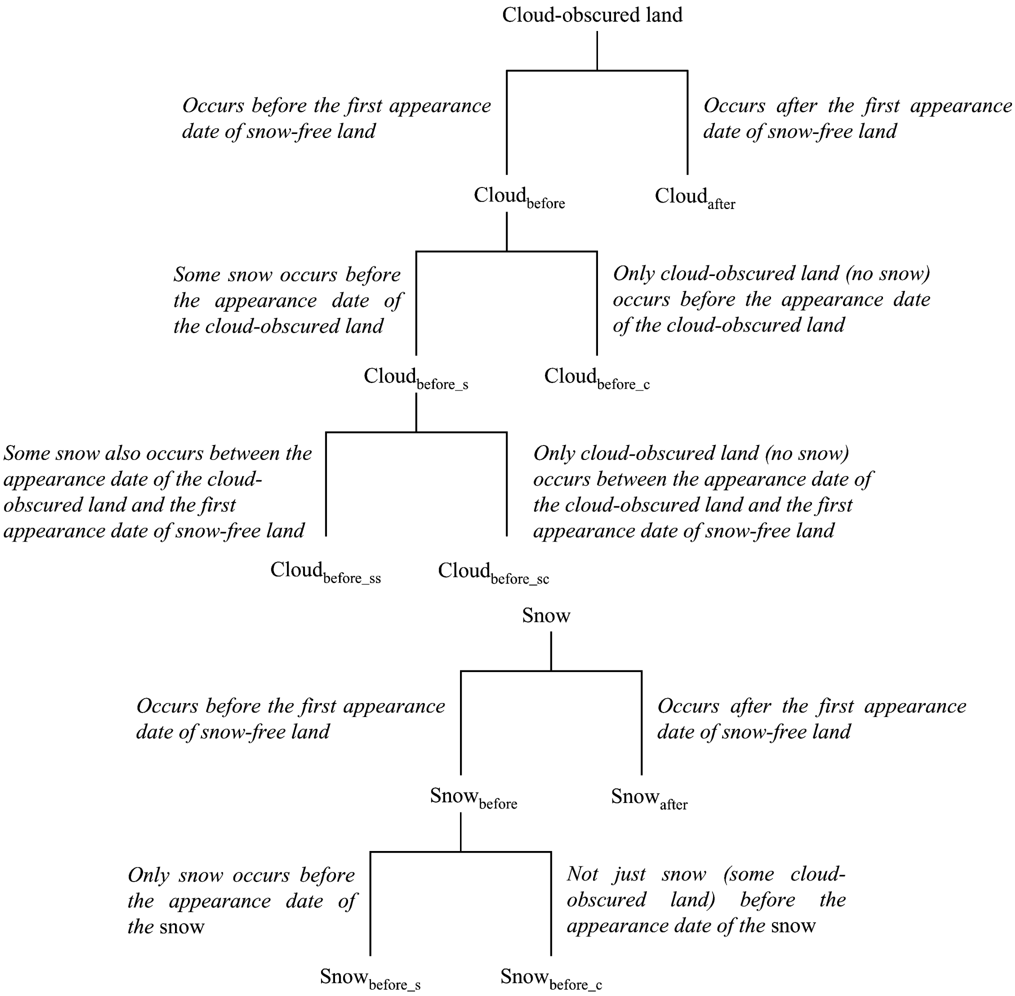

Figure 3. Reclassification of cloud-obscured land and snow; cloud-obscured land was reclassified into Cloud$_{after}$, Cloud$_{before_c}$, Cloud$_{before_ss}$ and Cloud$_{before_sc}$ snow was reclassified into Snow$_{after}$, Snow$_{before_s}$ and Snow$_{before_c}$

Table III. Reclassified classes of both snow and cloud-obscured land and corresponding trajectory examples

Classes	Trajectory examples
Cloud$_{after}$	$S^{3\cdot15} \rightarrow S^{3\cdot16} \rightarrow S^{3\cdot17} \rightarrow S^{3\cdot18} \rightarrow S^{3\cdot19} \rightarrow L^{3\cdot20}_{first} \rightarrow C^{3\cdot21}_{after} \rightarrow \ldots \rightarrow L^{6\cdot10}$
Cloud$_{before_c}$	$C^{3\cdot15}_{before\_c} \rightarrow C^{3\cdot16}_{before\_c} \rightarrow L^{3\cdot17}_{first} \rightarrow L^{3\cdot18} \rightarrow L^{3\cdot19} \rightarrow L^{3\cdot20} \rightarrow L^{3\cdot21} \rightarrow \ldots \rightarrow L^{6\cdot10}$
Cloud$_{before_ss}$	$S^{3\cdot15} \rightarrow S^{3\cdot16} \rightarrow C^{3\cdot17}_{before\_ss} \rightarrow S^{3\cdot18} \rightarrow S^{3\cdot19} \rightarrow S^{3\cdot20} \rightarrow L^{3\cdot21}_{first} \rightarrow \ldots \rightarrow L^{6\cdot10}$
Cloud$_{before_sc}$	$S^{3\cdot15} \rightarrow S^{3\cdot16} \rightarrow S^{3\cdot17} \rightarrow C^{3\cdot18}_{before\_sc} \rightarrow C^{3\cdot19}_{before\_sc} \rightarrow L^{3\cdot20}_{first} \rightarrow L^{3\cdot21} \rightarrow \ldots \rightarrow L^{6\cdot10}$
Snow$_{after}$	$S^{3\cdot15} \rightarrow S^{3\cdot16} \rightarrow S^{3\cdot17} \rightarrow L^{3\cdot18}_{first} \rightarrow S^{3\cdot19}_{after} \rightarrow L^{3\cdot20} \rightarrow L^{3\cdot21} \rightarrow \ldots \rightarrow L^{6\cdot10}$
Snow$_{before_s}$	$S^{3\cdot15}_{before\_s} \rightarrow S^{3\cdot16}_{before\_s} \rightarrow S^{3\cdot17}_{before\_s} \rightarrow L^{3\cdot18}_{first} \rightarrow L^{3\cdot19} \rightarrow L^{3\cdot20} \rightarrow L^{3\cdot21} \rightarrow \ldots \rightarrow L^{6\cdot10}$
Snow$_{before_c}$	$S^{3\cdot15}_{before\_c} \rightarrow S^{3\cdot16}_{before\_c} \rightarrow C^{3\cdot17} \rightarrow S^{3\cdot18}_{before\_c} \rightarrow S^{3\cdot19}_{before\_c} \rightarrow L^{3\cdot20}_{first} \rightarrow L^{3\cdot21} \rightarrow \ldots \rightarrow L^{6\cdot10}$

In trajectory examples, S is snow; C is cloud-obscured land; L is snow-free land; L_{first} is the snow-free land, which appears for the first time in this trajectory.

denotes the fact that the cloud-obscured land appears 'before' the first appearance date of snow-free land. The first 's' of this subscript denotes the fact that some snow exists before the appearance date of the Cloud$_{before_ss}$ and the second 's' denotes the fact that some 'snow' also occurs between the appearance date of the Cloud$_{before_ss}$ and the first appearance date of snow-free land.

Cloud$_{before_sc}$ appears before the first appearance date of snow-free land. At the same time, some snow occurs before the appearance date of the Cloud$_{before_sc}$, but only cloud-obscured land (no snow) occurs between the appearance date of the Cloud$_{before_sc}$ and the first appearance date of snow-free land (C$_{before_sc}$ in the trajectory example in Table III, Figure 3). Subscripts 'before' and the first 's' are the same as those of Cloud$_{before_ss}$. Subscript 'c' denotes the fact that only cloud-obscured land (no snow) occurs between the appearance date of the Cloud$_{before_sc}$ and the first appearance date of snow-free land.

Snow$_{after}$ occurs after the first appearance date of snow-free land (S$_{after}$ in the trajectory example in Table III, Figure 3). Subscript 'after' denotes the fact that the snow occurs 'after' the first appearance date of snow-free land.

Snow$_{before_s}$ occurs before the first appearance date of snow-free land and only snow falls prior to the appearance date of the Snow$_{before_s}$ (S$_{before_s}$ in the

DOI: 10.1002/hyp

trajectory example in Table III, Figure 3). Subscript 'before' denotes the fact that the snow occurs 'before' the first appearance date of snow-free land, subscript 's' denotes the fact that 'only snow' exists before the appearance date of the $Snow_{before\_s}$.

$Snow_{before\_c}$ appears before the first appearance date of snow-free land and not just snow (some cloud-obscured land) falls before the appearance date of the $Snow_{before\_c}$ (S_{before_c} in the trajectory example, Figure 3). Subscript 'before' is the same as that of $Snow_{before\_s}$, subscript 'c' denotes the fact that 'not just snow (some cloud-obscured land)' exists before the first appearance date of the $Snow_{before\_c}$.

Determination of snow cover status of reclassified classes. Seasonal snow cover generally begins to melt from the maximum snow cover at the beginning of the snowmelt season. All snow cover on the date of maximum snow cover can be considered as seasonal snow cover. The process of seasonal snow cover melting can be considered as the gradual disappearance of this snow cover.

In the context of constructing a snow cover change trajectory, a typical seasonal snow cover change trajectory without the impact of temporary snow cover and cloud cover should be as follows: snow cover exists continuously before the first appearance date of snow-free land and the surface land cover at this site will be snow-free land after that date. Thus, if snow cover exists continuously before the first appearance date of snow-free land in a snow cover change trajectory at a site, all snow cover before that date should be seasonal snow cover. If snow cover appears after that date, it means that seasonal snow cover has melted completely at that site and the snow cover should then be considered as temporary snow cover.

$Cloud_{after}$ occurs after the first appearance date of snow-free land, it can only be assigned as temporary snow cover or snow-free land on the ground.

The snow cover status in the areas covered by $Cloud_{before\_c}$ cannot be determined based on snow cover change trajectory analysis. No snow in these areas appears before the first appearance date of snow-free land. One cannot estimate whether the surface land cover is snow cover or not in these areas. Thus, one cannot determine whether seasonal snow cover exists in these areas without additional information. In this work elevation conditions are employed to determine the status of this kind of cover type.

$Cloud_{before\_ss}$ can be extrapolated as seasonal snow cover. In general, $Cloud_{before\_ss}$ appears alternatively with $Snow_{before\_c}$ before the first appearance date of snow-free land in a trajectory and it is normal for $Snow_{before\_c}$ to occur frequently in this trajectory over the snowmelt season. At the same time, $Snow_{before\_c}$ appears at least once after the appearance date of $Cloud_{before\_ss}$. Under these conditions, it is hypothesized that there is a high probability that the $Cloud_{before\_ss}$ is snow on the ground; thus $Cloud_{before\_ss}$ can be extrapolated as snow cover. Only $Cloud_{before\_ss}$ and $Snow_{before\_c}$ can exist before the appearance date of $Cloud_{before\_ss}$ in a trajectory. Since $Cloud_{before\_ss}$ can be assigned as snow cover as discussed above, all surface land cover types should be snow before the appearance date of the $Cloud_{before\_ss}$. Therefore, the $Cloud_{before\_ss}$ can be assigned as seasonal snow cover.

$Cloud_{before\_sc}$ can be assigned as seasonal snow cover. In fact $Cloud_{before\_sc}$ only appears between the last appearance date of $Snow_{before\_s}$ or $Snow_{before\_c}$ and the first appearance date of snow-free land in a trajectory. The surface land cover types can only be cloud-obscured land cover during this period. This situation will generally not last for a long period of time (the period was less than 4 days in more than 85% of snow cover change trajectories, where $Cloud_{before\_sc}$ existed, according to the statistics in the study area). Since the area was recently covered by snow, it is hypothesized that there is a high probability that the $Cloud_{before\_sc}$ is snow cover. Before the appearance of a $Cloud_{before\_sc}$ in a trajectory, only $Snow_{before\_s}$, $Snow_{before\_c}$, $Cloud_{before\_ss}$ and $Cloud_{before\_sc}$ can occur. Since both $Cloud_{before\_ss}$ and $Cloud_{before\_sc}$ can be assigned as snow cover as discussed above, all surface land cover types will be snow before the first appearance date of the $Cloud_{before\_sc}$ in this trajectory. Therefore, this $Cloud_{before\_sc}$ can be assigned as seasonal snow cover.

$Snow_{after}$ can be assigned as non-seasonal snow cover, and $Snow_{before\_s}$ and $Snow_{before\_c}$ can be assigned as seasonal snow cover. Since $Snow_{after}$ occurs after the first appearance date of snow-free land, it can be assigned as temporary snow cover. $Snow_{before\_s}$ exists continuously before the first appearance date of snow-free land in a trajectory. Thus, it should be considered as seasonal snow cover. Only $Cloud_{before\_ss}$ and $Snow_{before\_c}$ can exist before the appearance date of $Snow_{before\_c}$. Since $Cloud_{before\_ss}$ can be assigned as snow cover as discussed above, all surface land cover types can be assigned as snow cover before the $Snow_{before\_c}$. Thus, the $Snow_{before\_c}$ can be assigned as seasonal snow cover.

Rules for operational classification of snow cover based on snow cover trajectory analysis. The reclassification of cloud-obscured land and snow and the determination of their corresponding snow cover status discussed above are based on snow cover change trajectories over the whole snowmelt season. The snow cover status of some reclassified classes cannot be determined without knowledge of all surface land covers over the whole snowmelt season. However, in practical application, snow cover depletion curves, which model daily snowmelt runoff, can only be determined through the snow cover maps from the beginning of the snowmelt season to a given date.

In order to make this method practical for application, four rules were derived to determine snow cover status of a pixel on a given date. According to these rules, the seasonal snow cover status of a pixel on a given date can be determined based on snow cover maps from the beginning of the snowmelt season to the given date. The four rules were deduced based on the

DOI: 10.1002/hyp

reclassification conditions of the reclassified classes and their corresponding snow cover status.

Rule I: *if snow-free land exists in the snow cover change trajectory from the beginning of the snowmelt season to a given date, the surface land cover of this pixel is assigned as non-seasonal snow cover regardless of whether the surface land cover of this pixel on the given date is snow or cloud-obscured land.* Only pixels classified as $Snow_{after}$ or $Cloud_{after}$ can meet the conditions of rule I, according to the earlier discussion. Because both $snow_{after}$ and $Cloud_{after}$ can only be considered as temporary snow or snow-free land, the surface land cover of this pixel should be non-seasonal snow cover.

Rule II: *if no snow-free land exists in the snow cover change trajectory from the beginning of the snowmelt season to a given date and if the surface land cover of this pixel on the given date is snow, the surface land cover of this pixel is assigned as seasonal snow cover.* Only pixels classified as $Snow_{before\_s}$ or $Snow_{before\_c}$ can meet the conditions of rule II, according to the earlier discussion. Because they can both be considered as seasonal snow cover, the surface land cover of this pixel should be seasonal snow cover.

Rule III: *if no snow-free land exists in the snow cover change trajectory from the beginning of the snowmelt season to a given date and if the surface land cover of this pixel on the given date is cloud-obscured land, but some snow exists over this period, the surface land cover of this pixel is assigned as seasonal snow cover.* Only pixels classified as $Cloud_{before\_ss}$ or $Cloud_{before\_sc}$ can meet the conditions of rule III, according to the earlier discussion. Because they can both be considered as seasonal snow cover, the surface land cover of this pixel should be seasonal snow cover.

Rule IV: *if no snow-free land exists in the snow cover change trajectory from the beginning of the snowmelt season to a given date and if the surface land cover of this pixel on the given date is cloud-obscured land and no snow exists during this period, the surface land cover of this pixel cannot be determined based on the snow cover change trajectory.* Only pixels classified as $Cloud_{before\_c}$ can meet the conditions of rule IV, according to the earlier discussion. As discussed earlier, its snow cover status cannot be determined based only on snow cover change trajectory analysis. Elevation is used to assist in determining the snow cover status of this cover type (see next section for details).

Processing flow for determining snow cover status of a pixel for a given date

A decision-tree-like processing flow is constructed to determine snow cover status of a pixel for a given date, using snow cover maps from the beginning of the snowmelt season to the given date (Figure 4). The rules, based on snow cover change trajectory analysis, are applied in sequential order. Because the snow cover status of a pixel under the conditions of rule IV cannot be determined based on snow cover change trajectory analysis alone, the method of 'critical' elevation analysis is used (Figure 4).

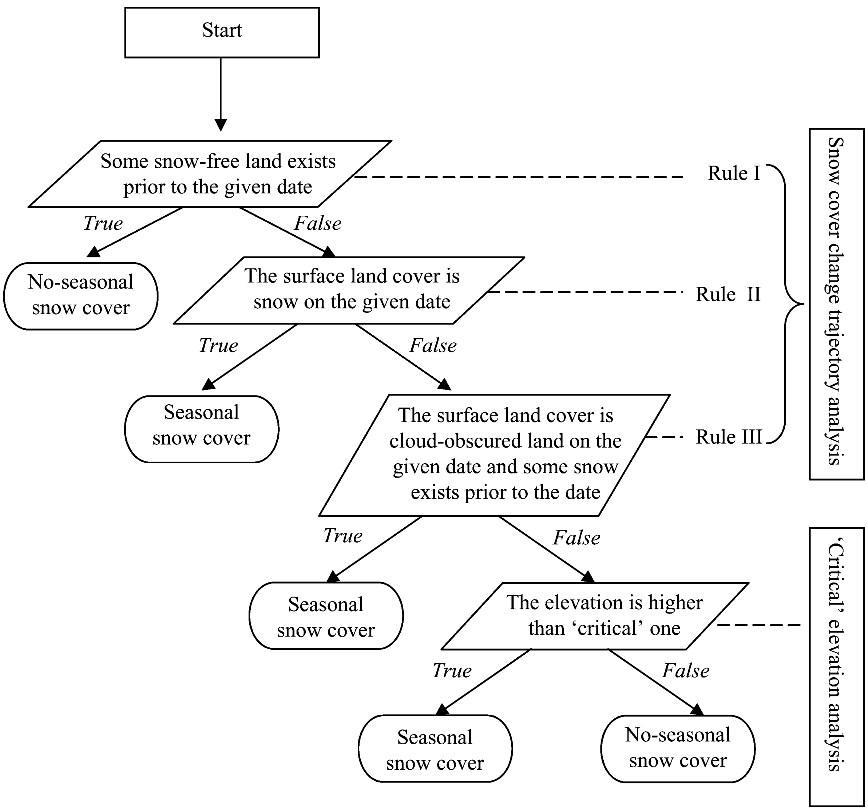

Figure 4. Processing flow of determining snow cover status of a pixel for a given date

DOI: 10.1002/hyp

The 'critical' elevation is specified as the minimum elevation in the reference area covered by seasonal snow cover. If the elevation at this pixel is higher than the 'critical' elevation its surface land cover is considered as seasonal snow cover, otherwise, it is not (Figure 4). The reference area includes all the seasonal snow cover area based on snow cover change trajectory analysis. The 'critical' elevation in the reference area can be measured based on digital elevation model (DEM) data using a geographical information system (GIS).

Mapping daily seasonal snow cover maps and snow cover depletion curves

When the status of seasonal snow cover of all pixels for a given date is determined, the determination of the seasonal snow cover map for this date is completed. After all seasonal snow cover maps for every date over a study period are completed, the process of daily seasonal snow cover mapping is over.

Based on daily seasonal cover maps over a study period, daily seasonal snow cover area percentage can be obtained directly. Thus, the snow cover depletion curves over this study period can be automatically produced based on these daily seasonal snow cover area percentages.

Comparison with high spatial resolution remote sensing products

It is impossible to obtain daily validation data to evaluate snow cover depletion curves. Therefore, in this study consistency evaluation is based on the comparison with high spatial resolution remote sensing data. Seasonal snow cover is grouped into three classes: seasonal snow cover from $Snow_{before}$ (including $Snow_{before\_s}$ and $Snow_{before\_c}$), seasonal snow cover from $Cloud_{before\_s}$ (including $Cloud_{before\_ss}$ and $Cloud_{before\_sc}$) and seasonal snow cover from $Cloud_{before\_c}$. This classification is used to evaluate the effectiveness of the two methods (snow cover trajectory analysis and 'critical' elevation analysis) that are used to determine snow cover status in this study.

Remote sensing data with high spatial resolution (15–30 m) discussed earlier are the main source of consistency evaluation data sets. It is impossible to use ground measurement data as validation data because of the inaccessibility of these alpine mountains in the study area. Remote sensing data with 15–30 m resolution can provide more detailed snow cover information than MODIS data (500 m resolution). At the same time, these data are easily obtained at minimum expense.

Terra ASTER data is used only for consistency evaluation of seasonal snow cover in cloud-free regions. Because ASTER data are at optical frequencies and pass the study area synchronously with MODIS, they are not used for the consistency evaluation of seasonal snow cover in cloud-obscured areas.

CBERS CCD data are used for consistency evaluation of seasonal snow cover in both cloud-free regions and cloud-obscured areas. Although CBERS also use optical sensors, they do not pass the study area synchronously with MODIS. Some cloud (e.g. altostratus), which move very quickly, appear frequently when there is no precipitation in alpine mountains. Thus, it is possible to locate areas where this kind of cloud exists when MODIS passes the study area, and the sky is clear when CBERS passes. Thus, the CBERS data in these areas can be used for consistency evaluation in cloud-obscured areas.

In order to improve the consistency evaluation of the test dataset, the selection of consistency evaluation data is based on three criteria: (1) there is no precipitation on the present and previous dates of consistency evaluation data. If the consistency evaluation data are CBERS data, some cloud should exist on the MODIS snow cover map on that date; (2) there is no obvious temporary snow cover on that day, which is determined by the visual comparison of MODIS composites on that day and on previous dates; and (3) the test data cover as much of the snowmelt season as possible. The dates of the selected data were 27 March, 12 May and 22 May, 2001. Thus, the accuracy of the seasonal snow cover maps for these three dates is assessed using the test data obtained. Unfortunately, we are unable to obtain suitable higher spatial resolution images for April 2001.

The percentage of correct seasonal snow cover samples to the total samples is taken as the accuracy index. A total of 100 sample points based on a stratified random sampling scheme for each of the three seasonal snow cover maps to be tested is generated. These sample points for each of these three seasonal snow cover maps are then overlaid on the three composites of CBERS CCD and Terra ASTER. A decision regarding seasonal snow cover at each of these sample points is made based on a visual interpretation of these composites. When the surface land cover of a sample is all snow on the consistency evaluation images for both the present and all previous dates, this sample is taken as seasonal snow cover, otherwise, it is not. The consistency evaluation data are then used to compute the accuracy index.

RESULTS

Daily seasonal snow cover maps

Figure 5 illustrates seasonal snow cover maps at 10-day intervals in 2000 and 2001. The outlines of seasonal snow covers distributed along a similar elevation and their patterns were very similar to those of local landforms. This consistency between the daily seasonal snow cover maps and the landscape physiography suggests that the former are approximating actual snow cover conditions accurately.

Table IV shows the seasonal snow cover accuracies which are consistent with those determined using a high spatial resolution dataset. The accuracies of total seasonal snow cover range from 87·0 to 91·0%. The accuracies of the seasonal snow cover from $Snow_{before}$ vary from 87·8 to 90·0%. The accuracies of the seasonal snow cover from $Cloud_{before\_s}$ are 93·3%. The accuracy of seasonal snow cover from $Cloud_{before\_c}$ is 72·7%.

DOI: 10.1002/hyp

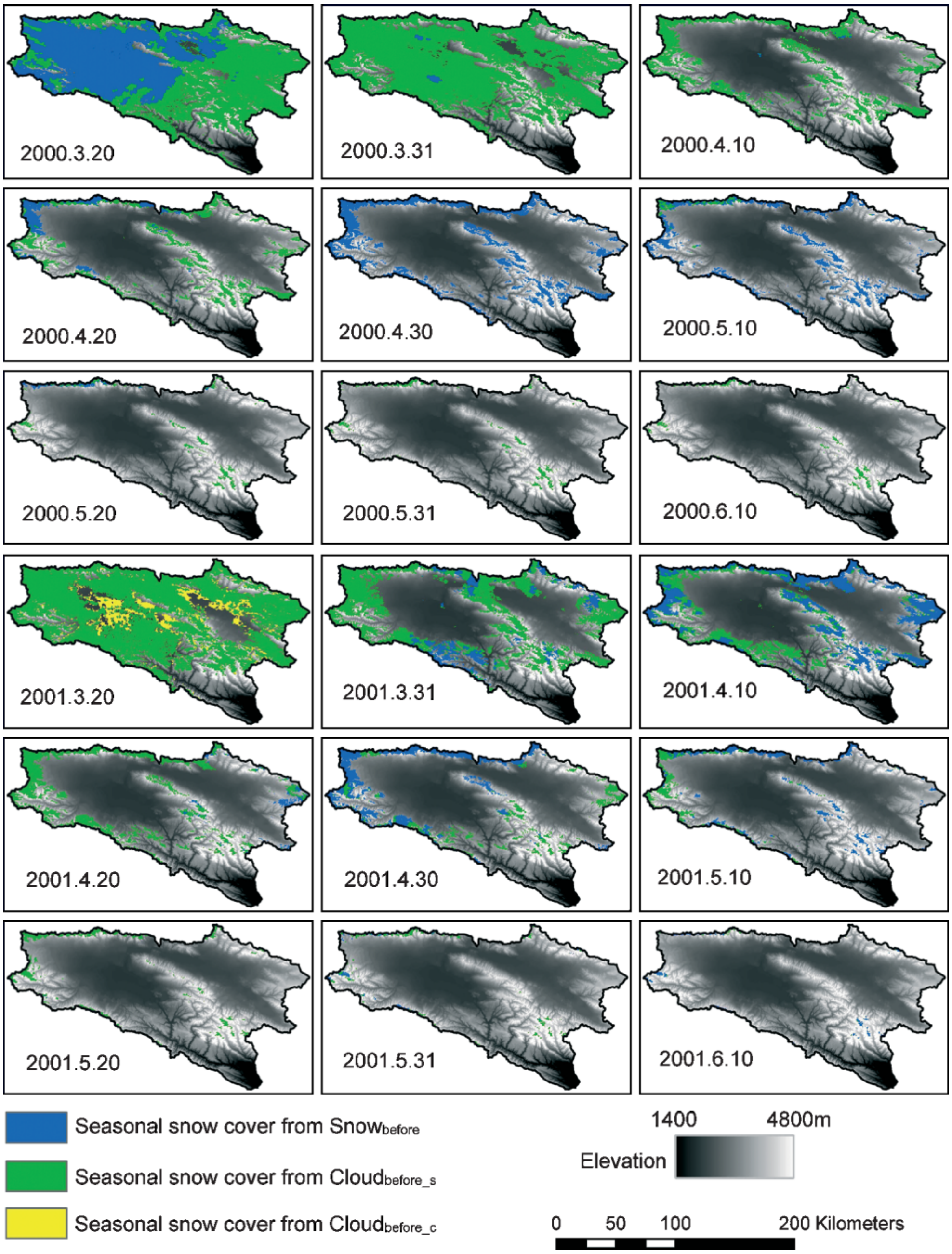

Figure 5. Seasonal snow cover maps every ten days in 2000 and 2001. Snow melted gradually and most had melted by 20 May. Its spatial pattern was similar to that of the local landform

Table IV. Accuracies of determining daily seasonal snow cover maps

Date	Seasonal snow cover from $Snow_{before}$	Seasonal snow cover from $Cloud_{before\_s}$	Seasonal snow cover from $Cloud_{before\_c}$	Total seasonal snow cover
27/03/2001	87·8%	93·3%	72·7%	87·0%
12/05/2001	90·0%	93·3%	—	91·0%
22/05/2001	89·0%	—	—	89·0%

The results show that the level of accuracy of seasonal snow cover based on snow cover trajectory analysis (seasonal snow cover from $Snow_{before}$ and $Cloud_{before\_s}$) is similar. At the same time, the accuracy of seasonal snow cover based on snow cover trajectory analysis is obviously higher than that of seasonal snow cover based on 'critical' elevation analysis (seasonal snow cover from $Cloud_{before\_c}$).

Snow cover depletion curves

Figure 6 demonstrates in general that seasonal snow cover decreased gradually during the snowmelt season in 2000 to 2005. The seasonal snow cover melted mainly in March and April. The melting of the seasonal snow cover was over by 20–31 May 2000, 2001, 2004 and 2005 and by 1–10 June 2002 and 2003. All these seasonal snow cover depletion processes are in agreement with

DOI: 10.1002/hyp

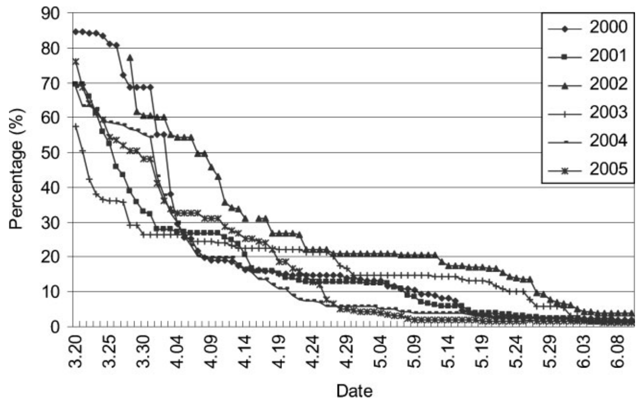

Figure 6. Snow cover depletion curves during the snowmelt season from 2000 to 2005. The percentages of seasonal snow cover decreased gradually, but non-uniformly

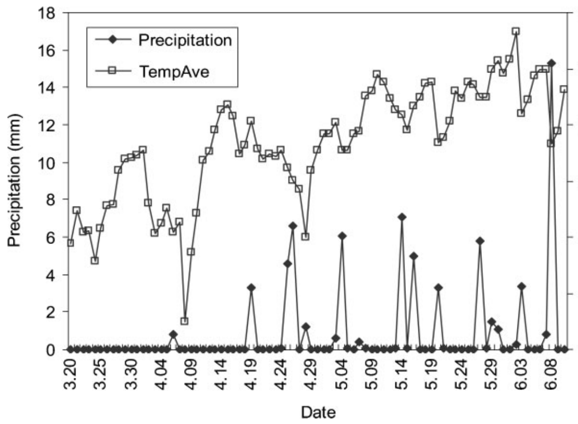

Figure 8. Daily average temperature (TempAve) and daily precipitation (Precipitation) at Bayanblak in 2001; temperature was low when precipitation peak appeared

the general conditions of historical snow cover depletion processes in the Chinese Tien Shan, China (Ma, 2002)

Although seasonal snow cover generally decreased gradually, depletion of seasonal snow cover varied greatly over the whole snowmelt season. For example, from 2–10 April, 22 April to 5 May and 13 to 16 May 2001, the depletion curves showed that seasonal snow cover melting nearly halted. This temporal variability of the rate of seasonal snow cover depletion was consistent with the time series of air temperature, as well as the appearance of temporary snow cover (Figure 7 and Figure 8).

In this study the changes in temperature and the appearance of temporary snow cover are both based on meteorological data. Daily average temperature is used as the index to illustrate temperature changes. 0 °C is taken as the 'critical' temperature when snow cover begins to melt (WinSRM, 2003).

Whether temporary snow cover appears or not is determined by the 'critical' temperature on the appearance dates of precipitation. If the temperatures on these dates are less than the 'critical' temperature, the precipitation can be taken as snowfall. Because the snowfall appears during the snowmelt season, it can be considered as temporary snow cover.

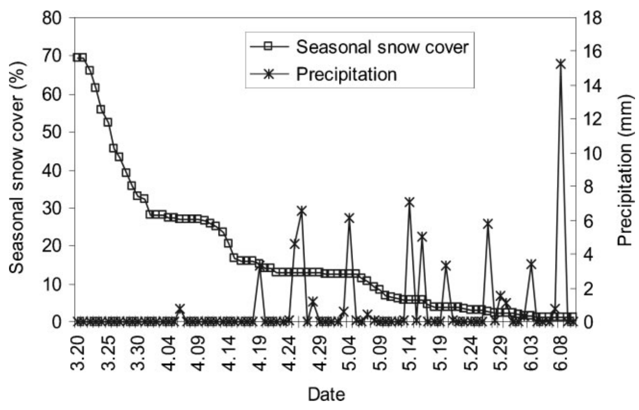

Figure 7. Snow cover depletion curves and daily precipitation from 20 March to 10 June 2001. The changes of seasonal snow cover depletion were in agreement with those of precipitation. When precipitation appeared, the melting of seasonal snow cover nearly stopped

The specific 'critical' temperatures in determining whether precipitation is temporary snow are specified as proposed by Martinec and Rango (1986). The 'critical' temperature starts at 3 °C in April at the beginning of the snowmelt season and deceases to 0·75 °C in July in the alpine basin Dischma in the Alps. WinSRM (2003) suggests that these 'critical' temperatures can be applicable to other basins because their seasonal trend is situated only within narrow ranges. Thus, the 'critical' temperatures for determining temporary snow used in this study are 3 °C and 2·3 °C in April and May, respectively; the latter value was obtained by linear interpolation of critical temperatures in April and July.

From 2 to 10 April in 2001, the halting of seasonal snow cover melting was in agreement with the temperature decrease during this period. Only a small mount of precipitation occurred during this period (Figure 7). Even if the precipitation was snowfall and taken as temporary snow cover, the impact of the temporary snow cover was minimal because of the small amount of precipitation.

The temperature during this period was much lower than that from 28 March to 1 April and was similar to that from 20–27 March (Figure 8). The daily average temperature recorded at the Bayanblak meteorological station varied from −12·8 to −2·1 °C from 2–10 April. Based on DEM and seasonal snow cover maps, the seasonal snow cover during this period was mainly distributed in an area with elevation ranging between 2500 and 4800 m. According to the elevation at the Bayanblak meteorological station (2458 m) and the commonly used temperature change rate of 0·65 °C per 100 m, the temperature in the area covered by the seasonal snow cover will range between −28·0 and −17·2 (elevation 4800 m) and −13·1 and −2·3 °C (elevation 2500 m). Snow cover would not melt at these kinds of temperatures.

Between 22 April and 5 May and between 13 and 16 May in 2001, halts in seasonal snow cover melting were in agreement with the appearance of temporary snow cover. Precipitation occurred on the 7 days between 22 April and 5 May and appeared every day between 13 and 16 May (Figure 8). If these particular precipitation

DOI: 10.1002/hyp

events were snowfall and taken as temporary snow cover, the seasonal snow cover melting would cease because of the appearance of temporary snow cover. Thus, seasonal snow cover depletion should stop.

Most precipitation in the area covered by seasonal snow cover during these two periods can be specified as snowfall, according to local temperature conditions. The daily average temperature at the Bayanblak meteorological station ranged between −5·0 and 5·2 °C from 22 April to 5 May and varied between 4·6 and 6·7 °C from 13–16 May (Figure 8). Based on DEM and seasonal snow cover maps, the seasonal snow cover between 22 April and 5 May was mainly distributed in an area with elevation ranging from 2800 m to 4800 m and that between 13 and 16 May was mainly located in an area with elevation ranging from 3100 m to 4800 m. According to the elevation at the Bayanblak meteorological station (2458 m) and the temperature change rate of 0·65 °C per 100 m, the temperature in the area covered by seasonal snow cover will range between −20·2 and −10·0 °C (elevation 4800 m) and −7·2 and −3·0 °C (elevation 2800 m) from 22 April to 5 May and vary between −10·6 and −8·5 °C (elevation 4800 m) and 0·4–2·5 °C (elevation 3100 m) from 13–16 May. In nearly all the areas with seasonal snow cover during these two periods the temperature was less than the 'critical' temperature (3 °C in April and 2·3 °C in May). Thus, these precipitation events can be considered as snowfalls. Since these snowfalls occurred during the snowmelt season, they can be considered as temporary snow cover.

Between 19 May and 10 June 2001, the snow cover depletion curves did not change with temperature changes or the appearance of precipitation (Figures 7 and 8). This is because the snowmelt season had almost ended and most seasonal snow cover had melted by 19 May.

DISCUSSION

The contribution of this method

Snow cover depletion curves can be produced automatically. The laborious process of selecting cloud free and temporary snow free images by the commonly-used interpolation method is thus not required. According to the analysis of snow cover change trajectories, a decision-tree-like processing flow is developed to determine snow cover status for a pixel on a given date. Through this processing flow, daily seasonal snow cover maps can be generated directly, using snow cover maps from the beginning of the snowmelt season to a given date with commonly used GIS or remote sensing (RS) processing software.

Snow cover depletion curves using this method are more accurate than those derived using interpolation methods because the curves can provide a more detailed depletion process of seasonal snow cover. Snow cover depletion curves based on interpolation methods cannot provide this detail because cloud free and temporary snow cover free images are often difficult to obtain. In general, the larger the study area, the lower the probability is of obtaining this kind of data. However, the proposed method takes the pixel as a unit when determining snow cover status. Thus, one can obtain all the cloud free and temporary snow cover free images for every pixel over a study period. Therefore, more detailed snow cover depletion curves can be produced.

The impact of the length of the snow cover map series

The accuracy of the seasonal snow cover map based on a number of short series of snow cover maps will be lower than that based on a long series of snow cover maps. If the series of snow cover maps is short, $Cloud_{before\_c}$ will exist. The snow cover status of $Cloud_{before\_c}$ is determined by 'critical' elevation analysis. This method assumes that all $Cloud_{before\_c}$ covered areas, where the elevation is higher than the 'critical' one, are considered as areas covered by seasonal snow cover. However, there are some areas where there is no seasonal snow cover, but elevation is higher than the 'critical' one (e.g. some quite steep areas), and these areas may also be assigned to the category of seasonal snow cover. Thus, the accuracy of seasonal snow cover from $Cloud_{before\_c}$ cannot be very high (this has been proven in this study). Therefore, the accuracy of total seasonal snow cover will be low when the length of the snow cover series is short.

Although the accuracy of the seasonal snow cover from $Cloud_{before\_c}$ was not very high, this will not impact the accuracy of seasonal snow cover maps very seriously over the entire snowmelt season. On the one hand, seasonal snow cover from $Cloud_{before\_c}$ only appeared at the beginning of the snowmelt season (Figure 9). On the other hand, the area covered by this kind of seasonal snow cover was limited. Only for a few days during the appearance dates of $Cloud_{before\_c}$, was the area about 8% of the total study area. On other days when $Cloud_{before\_c}$ appeared, seasonal snow cover from $Cloud_{before\_c}$ was less than 5% of the total study area (Figure 9).

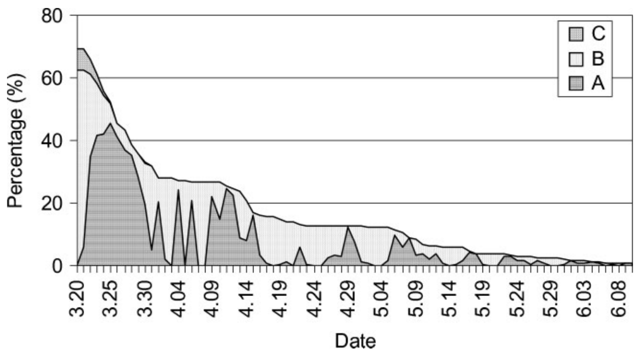

Figure 9. Components of seasonal snow cover during snowmelt season in 2001. A, B and C are percentages of seasonal snow cover from $Snow_{before}$, $Cloud_{before\_s}$, $Cloud_{before\_c}$, respectively. The seasonal snow cover from $Cloud_{before\_c}$ appeared at the beginning of the snowmelt season and its percentage was limited

DOI: 10.1002/hyp

The impact of the original snow cover map misclassification

Because the mapping of seasonal snow cover using this method is based on a snow cover change trajectory analysis, and not just based on an individual snow cover map, the impact of misclassifications on the results of seasonal snow cover mapping is generally not serious unless misclassifications are too frequent. First, if $Cloud_{after}$ is misclassified as snow or $Snow_{after}$ is misclassified as cloud-obscured land, this will not impact the results of seasonal snow cover mapping. Under this kind of condition, $Cloud_{after}$ will become $Snow_{after}$ and $Snow_{safter}$ will become $Cloud_{after}$. As discussed earlier, the status of both classes is considered to be non-seasonal snow cover.

Secondly, if $Cloud_{before\_c}$ is misclassified as snow, it will impact the results of seasonal snow cover mapping, but not very seriously over the entire snowmelt season. If a $Cloud_{before\_c}$ is misclassified as snow, it will become $Snow_{before\_c}$. As discussed earlier, the snow cover status of $Snow_{before\_c}$ can be determined based on snow cover change trajectory analysis; the snow cover status of $Cloud_{before\_c}$ can only be determined based on a 'critical' elevation analysis and the accuracy of seasonal snow cover from $Cloud_{before\_c}$ is relatively low. Therefore, these kinds of misclassifications will impact the results of final seasonal snow cover maps. However, $Cloud_{before\_c}$ only occurs at the beginning of the snowmelt season and its area is limited. Thus, the misclassification of $Cloud_{before\_c}$ will not impact the seasonal snow cover mapping seriously over the entire snowmelt season.

Thirdly, if $Cloud_{before\_ss}$ or $Cloud_{before\_sc}$ is misclassified as snow, these misclassifications will not impact the results of seasonal snow cover mapping. If $Cloud_{before\_ss}$ or $Cloud_{before\_sc}$ is misclassified as snow, the surface land cover will become $Snow_{before\_c}$ or $Snow_{before\_s}$. Because the snow cover status of all these four reclassified classes can be considered as seasonal snow cover, these kinds of misclassifications will not impact the final seasonal snow cover maps.

Finally, if $Snow_{before\_s}$ or $Snow_{before\_c}$ is misclassified as cloud-obscured land, these misclassifications will impact the results of seasonal snow cover mapping obviously when misclassifications are frequent in a snow cover change trajectory. If the misclassifications are so frequent that all $Snow_{before\_s}$ or $Snow_{before\_c}$ are misclassified as cloud-obscured land in a snow cover change trajectory, both $Snow_{before\_s}$ and $Snow_{before\_c}$ will become $Cloud_{before\_c}$ in this trajectory. As discussed earlier, the snow cover status of $Cloud_{before\_c}$ can only be determined based on a 'critical' elevation analysis and the accuracy of seasonal snow cover from $Cloud_{before\_c}$ is relatively low. Thus, these kinds of misclassifications can obviously impact the final seasonal snow cover maps.

If $Snow_{before\_s}$ or $Snow_{before\_c}$ in a snow cover change trajectory are not all misclassified as cloud-obscured land, the misclassified $Snow_{before\_s}$ or $Snow_{before\_c}$ will become $Cloud_{before\_ss}$ or $Cloud_{before\_sc}$. Because the snow cover status of all these four reclassified classes can be considered as seasonal snow cover, these kinds of misclassifications will not impact the final seasonal snow cover maps.

The impact of long periods of cloud cover

There could be weeks of cloud cover in many mountainous regions, which could easily lead to a delay in the initial observation of snow-free land. However, this kind of delay will not impact the accuracy of snow cover depletion curves greatly. This kind of cloud-obscured land is mainly related to $Cloud_{before\_sc}$. On the one hand, this kind of cloud-obscured land in most snow cover change trajectories does not last for a long time. According to the statistics in the study area, this kind of cloud-obscured land lasted less than 4 days in more than 85% of these trajectories.

On the other hand, even if this kind of cloud-obscured land lasts for a long period of time, the snow cover depletion curves will, in general, not be impacted seriously. When long periods of cloud cover occur, the temperature will normally drop. The lower temperature will lead to the seasonal snow cover melting ceasing or decreasing. Therefore, most cloud-obscured land over this period can be estimated as seasonal snow cover. Thus, the delay in the initial observation of snow-free land will not be too great. Furthermore, with the proposed methods, long periods of this kind of cloud cover will not greatly impact the accuracy of a snow cover depletion curve.

CONCLUSION

This study has developed a methodology to produce daily seasonal snow cover maps directly using optical remote sensing data with high temporal resolution so that accurate snow cover depletion curves can be produced automatically. The general idea of this method is that the snow cover existing on some dates at a site can provide information for determining the presence of snow cover on other dates at the same site. According to an analysis of snow cover change trajectories, a decision-tree-like processing flow is developed to determine the snow cover status for a pixel on a given date by using snow cover maps from the beginning of the snowmelt season to the given date. Temporary snow cover can be eliminated and seasonal snow cover in cloud-covered area can be extrapolated directly when mapping daily seasonal snow cover maps. Thus, accurate snow cover depletion curves can be produced automatically.

A case study based on Terra MODIS snow cover map products (MOD10A1) using this method was conducted in the lower and middle reaches of the Kaidu River Watershed (19 000 km^2) in the Chinese Tien Shan, Xinjiang Uygur Autonomous Region in China. Remote sensing data (CBERS CCD data with 19·5 m resolution and Terra ASTER data with 15 m resolution) were used to validate the results. This study shows that the seasonal snow cover classification was consistent with

DOI: 10.1002/hyp

that determined using a high spatial resolution dataset, with an accuracy of 87–91%. The snow cover depletion curves clearly reflected the impact of temperature variations and the appearance of temporary snow cover on snow cover melting. Interpolation methods use cloud-free and temporary snow free snow cover maps to map snow cover depletion curves. In general there are only limited cloud-free and temporary snow free snow cover maps available, thus, the snow cover depletion curve produced cannot capture detailed variations related to temperature variations and the appearance of temporary snow cover.

Results indicate that the proposed approach is successful in producing accurate snow cover depletion curves automatically using optical remote sensing data with high temporal resolution. With the availability of snow cover maps with high temporal resolution such as MODIS snow cover map products (MOD10A1), this method will be very helpful in producing accurate snow cover depletion curves for water-management applications of snow hydrology.

In this study, not all seasonal snow cover can be determined based only on a snow cover change trajectory analysis, and some were determined based on a 'critical' elevation analysis. The accuracy of the seasonal snow cover based on a 'critical' elevation analysis was clearly lower than that based on snow cover change trajectory analysis. However, according to this study, the relatively low accuracy of seasonal snow cover based on 'critical' elevation analysis will not impact the accuracy of the snow cover depletion curves seriously over the whole snowmelt season because seasonal snow cover based on 'critical' elevation analysis appeared only at the start of the snowmelt season, and the area where seasonal snow cover based on a 'critical' elevation analysis occurred was limited.

ACKNOWLEDGEMENTS

This study is supported by the 973 Program (2006CB701305), China National Natural Science Foundation (40101028), Pioneer Project of Institute of Geographical Sciences and Natural Resources Research, Chinese Academy of Sciences and the 'One-Hundred Talents Program' of the Chinese Academy of Sciences. Constructive criticism and comments from the anonymous referees are also acknowledged.

REFERENCES

Akyürek Z, Şorman AÜ. 2002. Monitoring snow-covered areas using NOAA-AVHRR data in the eastern part of Turkey. *Hydrological Sciences Journal* **47**: 243–252.

Baumgartner MF, Martinec J, Seidel K. 1986. Large-area deterministic simulation of natural runoff from snowmelt based on Landsat MSS data. *IEEE Transactions on Geoscience and Remote Sensing* **24**: 1013–1017.

Baumgartner MF, Seidel K, Martinec J. 1987. Toward snowmelt runoff forecasts based on multisensor remote-sensing information. *IEEE Transactions in Geoscience and Remote Sensing* **25**: 746–50.

Baumgartner MF, Rango A. 1995. A microcomputer-based alpine snow cover analysis system. *Photogrammetric Engineering & Remote Sensing* **61**: 1475–1486.

Congalton RG, Green K. 1999. *In Assessing the Accuracy of Remotely Sensed Data: Principles and Practices*. Lewis Publishers: Boca Raton; 43–64.

Engman ET, Gurney RJ. 1991. *Remote Sensing in Hydrology.* Chapman and Hall: London; 66–73.

Ferguson RI. 1999. Snowmelt runoff models. *Progress in Physical Geography* **23**: 205–227.

Guneriussen T, Johnsen H. 2003. Fully polarimetric airborne SAR and ERS SAR observations of snow: Implications for selection of ENVISAT ASAR modes. *International Journal of Remote Sensing* **24**: 3839–3854.

Guneriussen T, Johnsen H, Lauknes I. 2001. Snow cover mapping capabilities using RADARSAT standard mode data. *Canadian Journal of Remote Sensing* **27**: 109–117.

Hall DK, Martinec J. 1985. *Remote Sensing of Ice and Snow*. Chapman and Hall: New York; 31–53.

Hall DK, Riggs GA. 2007. Accuracy assessment of the MODIS snow-cover products. *Hydrological Processes* **21**: 1534–1547.

Koskinen J, Metsamaki S, Grandell J, Janne S, Matikainen L, Hallikainen M. 1999. Snow monitoring using radar and optical satellite data. *Remote Sensing of Environment* **69**: 16–29.

Ma H. 2002. *In Remote sensing snow hydrology in Western Tien Shan.* Doctoral thesis of Chinese Academy of Sciences, 15–40 (in Chinese).

Martinec J. 1975. Snowmelt-runoff model for stream flow forecasts. *Nordic Hydrology* **6**: 145–154.

Martinec J, Rango A. 1986. Parameter values for snowmelt runoff modeling. *Journal of Hydrology* **84**: 197–219.

Mertens B, Lambin EF. 2000. Land-cover-change trajectories in southern Cameroon. *Annals of the Association of American Geographers* **90**: 467–494.

Mognard NM, Grippa M, LeToan T, Kelly REJ, Chang ATC, Josberger EG. 2004. Comparison of AMSR-E and SSM/I snow parameter retrievals over the Ob river basin. *IEEE International Geoscience and Remote Sensing Symposium Proceedings*, Vols (1–7); 3713–3713.

Nagler T, Rott H. 1998. SAR tools for snowmelt model. *International Geoscience and Remote Sensing Symposium (IGARSS' 98),* Seattle, WA, IEEE: New York.

Petit CC, Scudder T, Lambin EF. 2001. Quantifying processes of land-cover change by remote sensing: resettlement and rapid land-cover changes in south-eastern Zambia. *International Journal of Remote Sensing* **22**: 3435–3456.

Rango A. 1996. Spaceborne remote sensing for snow hydrology application. *Hydrological Sciences Journal* **41**: 477–494.

Ranzi R, Grossi G, Bacchi B. 1999. Ten years of monitoring areal snowpack in the Southern Alps using NOAA-AVHRR imagery, ground measurements and hydrological data. *Hydrological Processes* **13**: 2079–2095.

Riggs GA, Hall DK, Salomonson V. 2006. MODIS Snow Product User Guide to Collection 5, NASA Goddard Space Flight Center, http:/modis-snow-ice.gsfc.nasa.gov.

Schaper J, Martinec J. Seidel K. 1999. Distributed mapping of snow and glaciers for improved runoff modeling. *Hydrological Processes* **13**: 2023–2031.

Seidel K, Ade F, Lichtengger J. 1983. Augmenting Landsat MSS data with topographic information for enhanced registration and classification. *IEEE Transactions on Geoscience and Remote Sensing* **21**: 252–258.

Shamir E, Georgakakos KP. 2007. Estimating snow depletion curves for American River basins using distributed snow modeling. *Journal of Hydrology* **334**: 162–173.

Storvold R, Malnes E. 2004. Snow covered area retrieval using ENVISAT ASAR wideswath in mountainous areas. *IEEE International Geoscience and Remote Sensing Symposium Proceedings,* Vols (1–7): 1845–1848.

Tekeli AE, Akyürek Z, Şorman AA, Şensoy A, Şorman AÜ. 2005. Using MODIS snow cover maps in modeling snowmelt runoff process in the eastern part of Turkey. *Remote Sensing of Environment* **97**: 216–230.

WinSRM. 2003. *WinSRM User's Manual*. Available at: http://hydrolab.arsusda.gov/cgi-bin/srmhome.

DOI: 10.1002/hyp